Lightweight Optical Wavelength Communications without a Laser in Space

D. A. Hazzard, J. A. MacCannell, G. Lee, C. D. Garrett, J. A. Payne, N. Dahlstrom, and T. M. Shay
New Mexico State University
Klipsch School of Electrical and Computer Engineering
MSC 3-O
Las Cruces, NM 88005
TEL (505)-646-4817
Email: tshay@nmsu.edu

Abstract

We will present a model for an earth-to-low-earth-orbit optical communications system. The system modeled herein is designed to offer a very lightweight, low power consumption, low data rate communications link from LEO satellites. A novel architecture for a free-space optical communications link is presented and analyzed. For the first time, a method that offers full-duplex communications on a single beam is presented. In addition, a novel data format for free-space optical communications is presented. In this system, both the laser and the downlink receiver are located on the ground. The optical elements located on the spacecraft are a simple uplink receiver and a retro-modulator. In fact, the laser transmitter for the system is a semiconductor device. We will present a simple feasibility model for the LOWCAL experiment that provides an estimate of the performance capability and identifies major system tradeoffs. Assuming a laser transmitter power of -7-dB and a communications data rate of 10-kbps, we expect link margins of 17 dB for the downlink. For the uplink, an SC-FSK format is proposed that is invisible to the downlink and provides a link margin of 20 dB.

Introduction

We present a model for an earth-to-low-earth-orbit (LEO) optical communications system; the planned experiment is called Lightweight Optical Wavelength Communications without a Laser in Space (LOWCAL.) The LOWCAL system modeled herein is designed to offer a very lightweight, low power consumption, low data rate communications link from LEO satellites. The system utilizes a novel architecture for a free-space optical communications link. The "Lightwire" concept provides for the first time full-duplex communications on a single beam. In addition, we propose utilizing for the first time a novel data format for free-space optical communications. The current proposed application is a ground-to-LEO link. These concepts however, are generally applicable to other free-space optical communications systems as well.

In this system, the laser and the downlink receiver are both located on the ground. The optical elements located on the spacecraft are the retro-modulator and a simple uplink receiver. Data rates on the order of 10-kbps are currently possible without taxing the current laser or modulator technology. In fact, the transmitter laser for such a system is a semiconductor device. The envisioned system would include a Faraday Anomalous Dispersion Optical Filter[1,2,3,4] (FADOF) in the receivers and tracking system to allow 24-hour operation of the system. We previously reported the first solar blind laser communications system utilizing a FADOF in the receiver.[5] The FADOF is an ultra-high background rejection optical filter developed at New Mexico State University that essentially prevents skylight from reaching the photodetector while transmitting 80% of the signal photons. Without a FADOF in the receiver the transmitted laser power would need to be increased by at least a factor of 4 for the acquisition to be feasible for daylight operation at a Zenith angle of $\pi/3$.

We present a simple feasibility model for the LOWCAL experiment that provides an estimate of the performance capability and identifies the major system tradeoffs. In our model we have calculated the required downlink receiver aperture, transmitter laser power, retro-modulator aperture, and both the downlink and the uplink signal-to-noise ratios. We have made allowances for the atmospheric scintillations in our model. We will first discuss the analysis of the downlink and then we will analyze the uplink.

LOWCAL Downlink

Nearly all of the optical communications experiments to date have utilized either On-Off Keying (OOK) or various coherent optical communications keying (PSK or FSK). We choose to employ for the first time Circularly Polarization Keying[6] (CPK). A block diagram of the system is shown in Fig. 1. The diode laser system transmits a constant average power beam to the spacecraft. The transmitted beam is directed through a quarter-wave plate ($l/4$ in Fig. 1) that will convert the linearly polarized laser beam into a circularly polarized beam. The laser beam is then directed through the aperture-sharing element (ASE) that is literally a mirror with a hole in it. The purpose of the aperture-sharing element is to separate the transmitted and returned beam paths. The transmitted beam is next directed through the hole in the mirror to the White Sands Missile Range Advanced Pointer and Tracker (WSMR APT) and then to the spacecraft. In circular polarization keying (CPK) the binary data is encoded in the polarization of the return beam. At the spacecraft, a liquid crystal (LCS) retro-modulator will flip the right-handed polarized transmitter light into left-handed for a “1”, while for a “0” the incident left-handed polarization is left unchanged. The liquid crystal retro- modulator acts exactly like a corner cube reflector, that is, the retro-modulator directs the beam incident on the spacecraft directly back to the transmitting telescope. Then the telescope

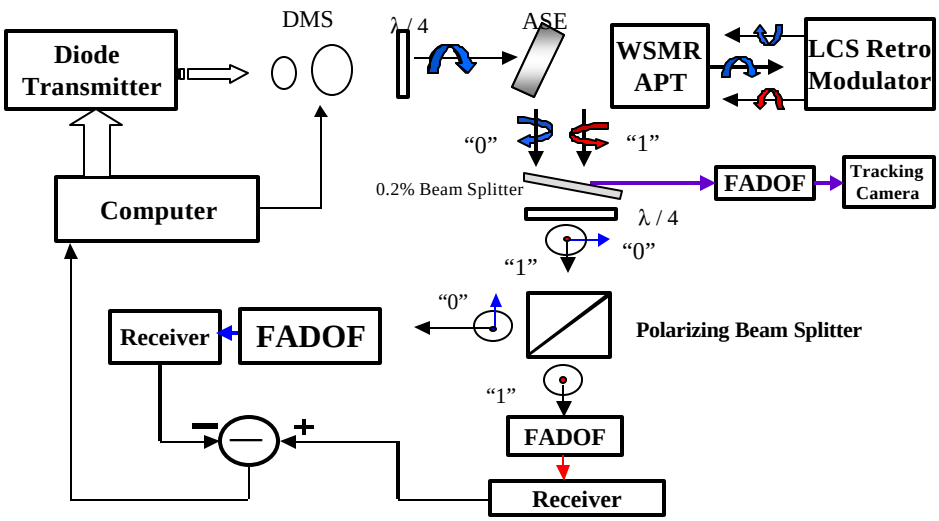

Fig. 1. LOWCAL block diagram

collects the downlink signal and directs the signal to the aperture-sharing element (ASE). The downlink signal is reflected by the ASE and directed to a beam splitter that sends 0.2% of the signal through a FADOF to the telescope's active tracking camera. Most of the return signal passes through the beam splitter to the receiver quarter-wave plate ($l/4$) that converts the left and right-hand circular polarized light into two orthogonal linear polarizations. The linear polarizations are then separated in the polarizing beam splitter shown in Fig. 1. The end result is the photons that constitute the "0's" are sent to one FADOF and photo-receiver and the photons that constitute the "1's" are sent to another FADOF and photo-receiver. Finally, these two signals are subtracted; hence, this new format is differential circular polarization keying (DCPK).

(Two additional advantages of CPK are; that, non-zero signals occur for both states and that the presence of "0's" and "1's" are both detected independently. If V_1 is subtracted from V_0, because $V_0 = -V_1$ at the threshold detector, the voltage difference between the high and low has doubled. Thus the received signal power is 6-dB higher than the received signal power for the more conventional On-Off Keying (OOK) utilizing the same peak transmitter power. In summary, DCPK is actually a differential form of CPK where the difference between the signal in the two circular polarizations are detected. Finally, we can easily distinguish between a long string of zeros and dropout since dropout occurs for signal levels near 0 volts and a zero corresponds to $-V_0$ volts. Thus, Lost, On and Off signals all have different signals. Therefore, we will name this format as CP-Lost-On-Off-Keying or CP-LOOK format. Note that the downlink is sensitive only to the average power received on each channel during a bit period; this will be utilized later. Another advantage of the CP-LOOK format is that since we always have power returning, a small percentage of the return signal can be directed to the our tracking error loop system without impacting either the signal coding or the significantly reducing the communications signal. CPK and DCPK are the first novel technical features of this system.

Simple Downlink Model

During the communications mode it is desirable to utilize a narrow transmit beam (~ 20-μradians) since this maximizes the power incident upon the spacecraft for a given transmitter power. The transmit beam divergence is limited by the atmosphere distortions, the atmospheric limited beam divergence, $\theta_{Transmit}$, is typically given by,

$$\theta_{Transmit} \approx \frac{l}{r_o} \qquad (1)$$

and

$$r_o \propto \lambda^{7/6} \qquad (2),$$

where r_o represents Freid's radius[7] and λ represents the wavelength of interest. A typical Fried radius at 532-nm is 5 cm and that corresponds to a Fried radius of 8.7 cm at 852-nm. Therefore, the beam divergence will typically be limited by the pointing accuracy of the telescope. We have chosen a beam divergence of approximately 20 microradians to be conservative.

According to the Shuttle Flight Dynamics Information Officer (FIDO)[8], the typical ephemeris uncertainty is 100-m downtrack. This corresponds to approximately 1/6-milliradian. The ephemeris uncertainty is approximately 10 times the communications beam width. Thus some search mechanism is necessary to acquire the spacecraft. Instead of mechanically scanning the receiver telescope beam, we will operate the system in two modes: first an acquisition mode, and secondly, as

soon as the signal is acquired, we will hand-off to the communications mode. To ensure rapid tracking convergence the acquisition mode transmitted beam will be wide (~ 0.4-milliradian) and a receiver integration time of a few milliseconds will be used. In the communications mode, the transmitted beam will be narrow (~20-μradians) and the integration time short to allow data rates of up to 10-kbps. The two operation modes have very different characteristics. Therefore the link equation is analyzed separately for the communications and the acquire modes.

Received Signal

The link equation for this system is

$$\text{Margin} = P_{\text{laser}} - L - P_{\min} \qquad (3),$$

where P_{laser} represents the transmitted laser power ,

P_{min} represents the minimum required signal power to close the link

L represents the total link loss, excluding the scintillation losses.

The 10-dB optical scintillation margin provided a BER of ~ 10^{-3} to 10^{-4} in the GOLD experiment[9]. Thus, we must have a link margin of greater than 10-dB. The sum of the modulator efficiency loss, L_{mod}, the atmospheric propagation loss, L_{atm}, the telescope loss, L_{T}, and the FADOF transmission loss, L_{FADOF}, add up to 9.5-dB. The signal intercept efficiency loss, L_{SIE}, is given by

$$L_{SIE} = -10\log\left(\frac{A}{R^2 \cdot \Delta\Omega}\right) \qquad (4),$$

where A represents the receiver area,
R the distance from the emitter to the receiver (between 300 and 600-km in a typical LEO[8]),
$\Delta\Omega$ represents the solid angle subtended by the transmitted beam.

$$R = \frac{h_{orbit}}{\cos(f)} \qquad (5),$$

where h_{orbit} represents the altitude of the orbit and ϕ represents the Zenith angle of the spacecraft.

The uplink solid angles are, $\Delta\Omega_{acquire} = 5.6\times10^{-7}$ sr and $\Delta\Omega_{comm} = 4\pi\times10^{-10}$ sr, for the acquisition and communications modes respectively. Furthermore, the solid angle of the return beam, DW_{return}, will typically be limited by the diffraction of the retromodulator optics. Assuming that the spacecraft is rolled through an angle, $\alpha = 34^{o}$ north to maximize the retro-modulator effective area seen from the ground station, then the effective area of the retro-modulator is,

$$A_{eff} = p \cdot \left(\frac{D_{retro}}{4}\right)^2 \cdot \cos(f - a) \qquad (6),$$

where D_{retro} represents the retro-modulator's diameter, respectively, while A_{eff} represents the retro-modulator's effective area as seen from the ground terminal.

Since the retro-modulator's effective area is an ellipse the diffraction limited return beam widths are,

$$J_{return\|} = 0.61 \cdot \frac{l}{D_{retro}} \qquad (7),$$

and

$$J_{return\perp} = 0.61 \cdot \frac{l}{D_{retro} \cdot \cos(f - a)} \qquad (8),$$

for the down-track and out-of-track angles, respectively.

Thus the diffraction limited return beam solid angle is,

$$\Delta\Omega_{return} = \pi \cdot \sin(\theta_{return\perp}) \cdot \sin(\theta_{return\|}) \qquad (9),$$

for small angles this is approximately,

$$\Delta\Omega_{return} \approx \pi \cdot \theta_{return\perp} \cdot \theta_{return\|} \qquad (10).$$

Substituting Eqs. 7 and 8 into Eq. 10 we obtain,

$$\Delta\Omega_{return} = \frac{\pi}{\cos(\phi - \alpha)} \cdot \left(\frac{0.61 \cdot \lambda}{D_{retro}} \right)^2 \qquad (11).$$

Thus returned signal power, P_s, is

$$P_s = P_{laser} \cdot \frac{(\eta_T \cdot \eta_{mod} \cdot \eta_{Atm})^2 \cdot \eta_{retro} \cdot \eta_{rbt} \cdot T_{FADOF} \cdot A_{retro} \cdot A_r}{R^4 \cdot \Delta\Omega_{up} \cdot \Delta\Omega_{return}} \qquad (12),$$

where η_T, η_{mod}, η_{Atm}, η_{retro}, and η_{rbt} represent the single pass telescope, modulator, atmospheric, retro-reflector, and receiver beam train losses, respectively. T_{FADOF} represents the signal transmission of the FADOF.

Substituting for R, A_{retro}, $\Delta\Omega_{up}$ and $\Delta\Omega_{return}$ in Eq. (12), we obtain,

$$P_s = P_{laser} \cdot (\eta_T \cdot \eta_{mod} \cdot \eta_{Atm})^2 \cdot \eta_{retro} \cdot \eta_{rbt} \cdot \left(T_{FADOF} \cdot \frac{A_r \cdot D_{retro}^4 \cdot \cos^4(\phi) \cdot \cos^2(\phi - \alpha)}{h_{orbit}^4 \cdot \pi \cdot (1.22 \cdot \lambda)^2 \cdot \theta_{Transmit}^2} \right) \qquad (13).$$

The return signal depends on the orbit altitude, h_{orbit}, to the fourth power as expected and also on the retro-modulator diameter to the fourth power, but the signal depends upon the Zenith angle to the sixth power. Thus, a small increase in spacecraft acquisition intercept angle yield large decreases in the required laser transmitter power. The maximum signal power, $P_s(\phi)$ occurs when the spacecraft is at

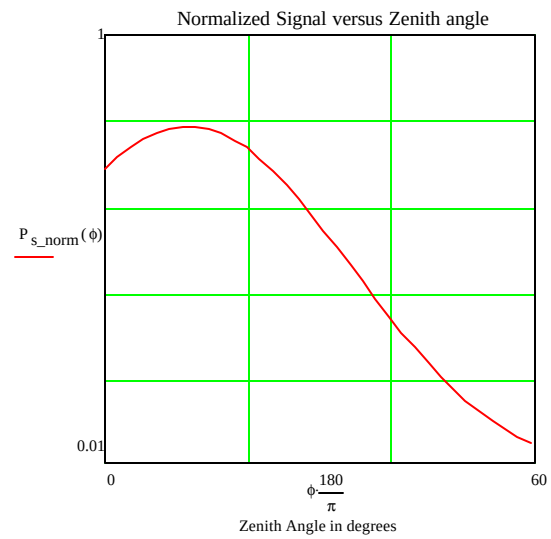

Zenith, the return signal power normalized to the maximum signal power, $P_s(0)$ is presented in Fig. 2.

Fig. 2, Normalized Received signal power versus spacecraft Zenith angle.

Fig. 2, clearly shows the dramatic dependence of the received signal power versus the spacecraft's Zenith angle. Note that at Zenith the signal power is 15 times stronger than the signal received at a Zenith angle of $\pi/3$. This variation can easily be handled by the receivers.

Table I. SYSTEM CHARACTERISTICS

Transmitter power	-7 dB (200 mW)
Receiver diameter	60 cm
Retro-modulator diameter	6-in
Data rate	10 kbps
Acquisition integration time	0.01 sec
Scintillation margin	10-dB
Atmospheric loss	3-dB
Modulator loss	1.4-dB
FADOF loss	1-dB
Retro-reflector loss	0.25-dB
Transmit beam divergence (Communications mode)	20-μradians
Transmit beam divergence (Acquisition mode)	420-μradians
Spacecraft intercept angle	π/3

Utilizing the system characteristics in Table I the calculated total round trip signal intercept efficiency losses at the spacecraft intercept angle are 80 and 104-dB for the communications mode and acquisitions modes, respectively. Note that the 24-dB difference in losses between the communications and acquire signal intercept losses is due only to the difference in transmit beam divergences for the two modes.

The expression for received optical signal power for the LOWCAL system is

$$P_s = 10\log\left(\frac{P_L}{\text{mW}}\right) - L \qquad (14),$$

where L represents the total optical link loss, given by

$$L = L_{\text{SIE}} + L_{\text{mod}} + L_{\text{atm}} + L_{\text{T}} + L_{\text{FADOF}} \qquad (15).$$

Thus, the expected received signal powers are 2.2 nW for the communications mode and 8 pW for the acquisition mode at a spacecraft intercept angle of π/3 from Zenith. In atmospheric communications the power must be increased to account for atmospheric scintillation. Therefore, we need to be certain that these received signal powers produce a signal-to-noise ratio that is at least 10-dB higher than the minimum signal-to-noise ratio required for the link.

Signal to Noise Ratio Analysis

The signal-to-noise ratio for a DCPK optical communications system in free space when inter-symbol interference can be neglected the signal-to-noise ratio is

$$SNR = \frac{\left(2 \cdot P_s \cdot (1 - 2 \cdot \boldsymbol{e}) \cdot R_{res}\right)^2}{\left(\begin{array}{l} 2 \cdot q \cdot G \cdot B \cdot P_s \cdot (1 - 2 \cdot \boldsymbol{e}) \cdot R_{res} + \\ 2 \cdot q \cdot G \cdot B \cdot P_{sky} \cdot R_{res} + 2 \cdot q \cdot G \cdot B \cdot I_D + \\ \dfrac{4 \cdot k_B \cdot T \cdot B \cdot F_t}{R_L} \end{array}\right)} \qquad (16),$$

where
R_{res} represents the responsivity of the photodetector,
ε represents the extinction coefficient of the retro-modulator,
q represents the electron charge,
G represents the photodetector internal gain,
B represents the electronic bandwidth, P_{sky} represents the total solar optical noise power that is incident upon the photodetector,

I_D represents the photodetectors dark current,
k_B represents Boltzman's constant,
T represents the load resistor's temperature,
R_L represents the load resistance,
F_t represents the noise Fig. of any electronic amplifiers.

Eq. (16) is valid as long as no optical preamplifier has been employed in the receiver and the photodetector is either a pin photodiode or a photo-multiplier tube. The first term in the denominator is the quantum noise term. The second term is due to solar background noise. The third term is due to the photodetector dark current, and the final term quantifies the resistor and electronic amplifier noises.

The extinction ratio of liquid crystal shutters fall off rapidly with frequency. It is the trade off between liquid crystal extinction ratio and link power penalty due to the non-zero extinction ratio that limits the data rate of our proposed system to 10 kbps. Finally, the measured extinction ratio at 10 kbps is less than 0.035.

The required signal to noise for a digital communications system is calculated using the complex error function. Assuming, that the probabilities of receiving a "1" and "0" are equal, and that the receiver threshold voltage is to set midway between, $V_1 + V_0 = 0$. A bit error rate of 10^{-6} requires the electrical SNR = 91. This is the minimum SNR that will provide a bit error rate of 10^{-6}. Therefore, a communications system in the field must exceed that SNR by at least one order of magnitude to overcome scintillation.

Next we will analyze the noise components of this system. The solar noise that is transmitted through the receiver and FADOF is given by

$$P_{\text{sky}} = \frac{\partial L_e}{\partial \lambda} \cdot \Delta\Omega_{\text{trans}} \cdot A_{\text{receiver}} \cdot \Delta\lambda_{\text{FADOF}} \cdot T_{\text{FADOF}} \cdot \eta_{\text{T}} \quad (17),$$

where $\frac{\partial L_e}{\partial \lambda}$ represents the spectral radiance of the blue sky,
$\Delta\lambda_{\text{FADOF}}$ represents the equivalent noise bandwidth of the FADOF,
T_{FADOF} represents the signal transmission of the FADOF.

The solar spectral radiance[10] at 1-micron is

$$\frac{\partial L_e}{\partial \lambda} = 10^3 \ \frac{\mu\text{W}}{\text{cm}^2 \cdot \text{sr} \cdot \mu\text{m}} \quad (18).$$

The spectral radiance of the blue sky remains roughly constant as long as the detector is pointing at a region of the sky that is greater than 10 degrees away from the sun. The solar noise incident upon the photodetector filtered by a FADOF is given by

$$P_{\text{sky}} = \frac{\partial L_e}{\partial \lambda} \cdot \Omega \cdot \Delta\lambda \cdot A_{\text{receiver}} \cdot T_{\text{FADOF}} \cdot \eta_{\text{T}}$$
(19),

where Ω represents the solid angle of the receiver,
$\Delta\lambda$ represents the optical bandpass of the FADOF (0.002-nm at 852-nm),
T_{FADOF} represents the signal transmission of the FADOF (80% at 852-nm.)

The total optical noise powers from the blue sky that reach the photodetectors are 5 fW and 1.4 pW for the communications and acquisition modes, respectively. The FADOF reduces the blue sky background to an insignificant level for both the daylight communications mode, where $\Delta\Omega = 1.27 \times 10^{-9}$ sr , and the daylight acquisition

mode, where $\Delta\Omega = 3.6\times 10^{-7}$ sr . Thus the FADOF makes it possible to operate in daylight as well as at night.
The characteristics of our photomultiplier based receivers are listed in Table II.

Table II. Receiver Characteristics

Responsivity	2,600 amps/watt
Quantum effficiency	0.005
Gain	750,000
Dark current	8 nA
Load resistance	100 kΩ
Bandwidth	20 kHz
Noise figure	~1

Utilizing the receiver characteristics calculated in Table II and P_{sky} for the communications mode, it is easily shown that the signal-to-noise ratio in the communications mode is to a good approximation shot noise limited, thus

$$SNR_{comm} = \frac{P_s \cdot \eta_{PMT}}{B \cdot h\nu} \qquad (20),$$

where η_{PMT} represents the photomultiplier quantum efficiency, hν represents the signal photon energy, and B represents the signal electronic bandwidth. Solving for the minimum required signal power,

$$P_{\min} = \frac{SNR_{\min}}{\eta_{PMT}} \cdot B \cdot h\nu \qquad (21).$$

Eq. 21 shows that P_{min} is proportional to SNR_{min} and the electronic bandwidth, B. The minimum required signal power is calculated

$$P_{min} = 45 \text{ pW} \qquad (22).$$

For a 200 mW transmitter, the calculated received power for a spacecraft intercepted at π/3 from Zenith is

$$P_s = 2.2 \text{ nW} \qquad (23).$$

The link margin, M, is

$$M = 10 \cdot \log\left(\frac{SNR_{comm}}{SNR_{\min}}\right) \qquad (24),$$

when the system is quantum noise limited, as in our case, this simplifies to,

$$M = 10 \cdot \log\left(\frac{P_s}{P_{\min}}\right) \qquad (25).$$

Substituting the calculated powers from Eqs. 22 and 23, the margin equals 17 dB. After subtracting the 10-dB that is required to overcome scintillation effects there remains a margin of 7 dB.

A single telescope is utilized to serve as both the transmitting and receiving antenna. This monostatic system is subject to strong interference due to transmitter light backscattered off near field aerosols. Therefore, we will operate with a 50% duty cycle to prevent the interference of near field backscattered transmitter light. However, this reduces the data rate by a factor of 2, so the electronic bandwidth is,

$$BW = 2 \cdot DR \qquad (26),$$

where DR = signal data rate.

At π/3 from Zenith, in the acquisition mode, both the signal shot noise and the photodetector noise terms contribute to yield a signal-to-noise ratio of,

$$SNR_{acquies} = 2{,}100 \qquad (27).$$

The higher losses during the acquisition mode are overcome by integrating over 10 milliseconds so that the acquisition can be completed quickly. This high signal-to-noise ratio should provide for rapid signal acquisition and tracking, so that the communications mode can start shortly after the intercept point is reached.

Finally, the liquid crystal shutter that is utilized is a phase-separated composite liquid crystal shutter[11] provided by Prof. Satyendra Kumar of Kent State University. The extinction ratio of liquid crystal shutters falls off rapidly with frequencies beyond 10 kHz. It is the trade off between liquid crystal extinction ratio and link power penalty due to the non-zero extinction ratio that limits the data rate of our proposed system to 10 kbps. The liquid crystal shutter system consumes 1/2 watt of electrical power for unbiased data.

Downlink Summary

The results presented in Table III assume a laser transmitter power of -7-dB, a communications data rate of 10-kbps, and an acquisition mode integration time of 10 milliseconds. The day and night signal-to-noise ratios are exactly the same due to the nearly 6 orders of magnitude rejection of the FADOF filter. In fact, during the communications mode, if the spacecraft flies directly in front of the sun so that the ground terminal is looking exactly into the sun, the signal-to-noise ratio is no longer shot noise limited. However, the signal-to-noise ratio only decreases by 5 dB.

TABLE III. Electrical Link Margins

		Comm		Acquire	
D_{retro} (in.)	Zenith angle	Day	Night	Day	Night
6	$\pi/3$	17	17	31	31

These results show clearly that a 6-inch diameter retro-modulator on board the satellite will close the link easily. The retro-modulator employs wide field lenses to increase its angular acceptance. A wide field-of-view retro-modulator is desirable because it reduces alignment sensitivity of the flight system, accurate pointing of a spacecraft requires significant flight system resources. In a very significant demonstration experiment that illustrated the potential of retro-modulator communications, Phillips Laboratory and Utah State University (AF/PL/USU)[12] used nine retro-modulators to achieve a field-of-view of $\pm\pi/4$ in their balloon experiments. We are designing a single retro-modulator that offers a field-of-view of greater than $\pm\pi/4$ and is very light-weight.

Comparison to Previous Retro-Modulated Communications

Currently, the only previous retro-modulator work that has been performed is the AF/PL/USU experiment[11]. A direct comparison of our work to that work is shown in Table IV.

Table IV. Comparison with the Other Experiment

	NASA/ NMSU	AF/PL/USU
Platform	Space Shuttle	Balloon
Altitude	320-km	32-km
Data rate	10-kbps	1.2-kbps
Receiver diameter	0.6-m	1.5-m
Modulator FOV	$\pm\pi/4$	$\pm\pi/4$
Modulator wt.	2 to 4-kg	28-kg
Modulator area	70 to 180-cm^2	1 to 10-cm^2
24 Hour Capability	Yes	No
Transmitter Power	0.2-W	5-W

As you can see from Table IV, our planned experiments should exceed the previous work in a number of categories. First, our platform is the space shuttle. Thus our link will be a factor of 10

higher and nearly a factor of 20 further away than the AF/PL/USU experiment. Second, we expect our data rate to be 8 times greater than AF/PL/USU experiment. Third, our receiver diameter is 0.6-m instead of 1.5-m. The modulator fields-of-view are comparable. The weight of our modulator should be an order of magnitude lower than their 28-kg. Our modulator effective area varies between 70 to 18 times the effective area of their modulator. We can provide 24-hour operation because of the use of a FADOF in the receiver. Our transmitter power should be over an order of magnitude lower than theirs, despite our extended performance.

The transmitter power required for the LOWCAL downlink at a spacecraft Zenith angle of $\pi/3$ with a bit error rate of 10^{-6} is plotted for 2 different receiver apertures in Fig. 3. In calculating the graphs in Fig. 3, the receivers' characteristics are listed in Table II, the two telescope diameters are 60-cm and 3.5-m. All of the remaining telescope characteristics are assumed identical to those listed in Table I. The minimum required transmitter power to provide a bit error rate of 10^{-6} is graphed on the vertical axis of Fig. 3.

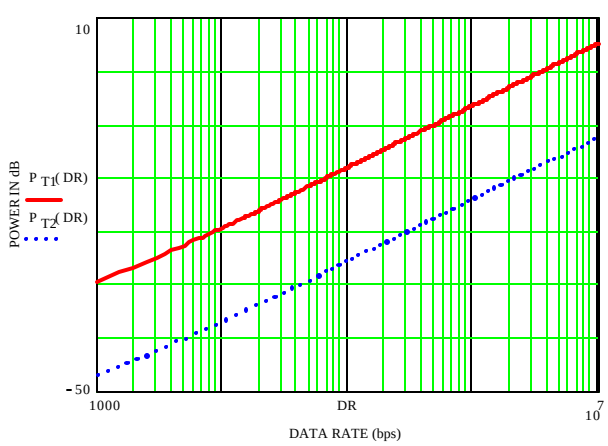

Fig. 3. Transmitter power versus data rate. In Fig. 3, P_{T1} and P_{T2} are the powers required for 60-cm diameter (solid curve) and 3.5 m diameter (dashed curve) telescopes, respectively.

LOWCAL UPLINK

It is desirable to have bi-directional communications for the proposed applications. An obvious means of doing this is to simply time multiplex the uplink and downlink modes. However, this reduces the data rate in both directions. Therefore, we invented a novel set of paired formats where the uplink data is invisible to the downlink and hence the uplink beam can simultaneously serve as the carrier for the downlink data. We have one optical beam that provides full-duplex operation without any penalty in data rate or signal-to-noise ratio.

We have named this the lightwire[14] concept. In this concept, we utilize different modulation schemes for the uplink and downlink. For the downlink, we utilize the DCPK modulation described in the previous section of this paper, but for the uplink we use sub-carrier FSK (SC-FSK) modulation with a small modulation index. The DCPK modulation format detects the difference between the total number of photons received in the two polarizations over one bit period. Because the SC-FSK modulation transmits a constant average power regardless of the data, the two modulation formats are transparent to one another. Hence, the uplink and downlink formats are invisible to each other. So we have full-duplex operation with one laser beam. At the spacecraft the photodetector converts the optical photons into a RF electrical signal and then at that point conventional FSK signal processing is utilized. Fig. 2 below illustrates the “Lightwire concept” operating in conjunction with the DCPK format. Note the system operates in two modes: talk and listen. During the talk mode the transmitted beam is on and the receiver is gated off and, conversely, during the listen mode, the receiver is gated on and the transmitter is off.

Finally, we have explicitly discussed the DCPK and SC-FSK Lightwire format pair. However, the results are generally applicable to any other format pair that meets the invisibility requirement. For example, an on-off keying downlink with a PSK or FSK uplink also constitute, a Lightwire format pair.

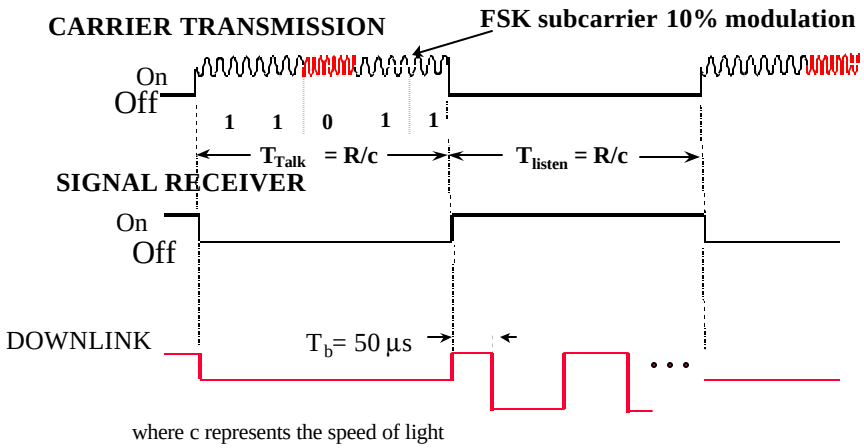

Fig. 2 Lightwire Format Pair

Uplink Model

A Lightwire system with a DCPK downlink is compatible with many possible uplink formats. Two obvious choices are PSK and FSK. PSK has the well known 3-dB signal-to-noise ratio advantage over FSK. However, the disadvantage of PSK is the need for an absolute phase reference or, alternatively, the first bit in any transmission block can provide the phase reference and differential PSK can be employed. To simplify the uplink receiver and to optimize the data throughput, we have chosen to employ SC-FSK for the uplink. For a receiver we employ a simple PLL tone decoder.

The optical power incident upon the spacecraft, P_r, is

$$P_r = I_i A_{\mathrm{PD}} \left[1 + m\cos\left(w_{\mathrm{FSK}} t\right)\right]$$

(28),

where P_r represents the received optical power at the spacecraft,
I_i represents the signal intensity incident upon the spacecraft,
m represents the modulation index,
w_{FSK} represents the subcarrier frequency.

The uplink signal-to-noise ratio is

$$\mathrm{SNR} = \frac{\frac{1}{2}\left(mP_r R_{\mathrm{PD}}\right)^2}{2qB\left(P_r R_{\mathrm{PD}} + I_{\mathrm{D}}\right) + \mathrm{RIN}\cdot B\left(P_r R_{\mathrm{PD}}\right)^2 + \frac{4k_B T\cdot B}{R_{\mathrm{L}}} F_t}$$

(29),

where q represents the electron charge,
B represents the electronic bandwidth,

R_{PD} represents the photodetector responsivity,
I_D represents the photodetector's dark current,
RIN represents the laser's relative intensity noise,
k_B represents Boltzman's constant,
T represents the temperature in degrees Kelvin,
R_L represents the load resistance,
F_t represents the noise figure of the amplifier.

For the designed receiver area of 4-cm^2 the received power at the spacecraft is 180-nW. Assuming a modulation index, m = 0.1, a photodetector responsivity, R_{PD} = 0.6 amps/watt, a data rate of 10-kHz, a relative intensity noise, RIN = -130-dB/Hz, and a load resister, R_L = 25-kΩ, the signal-to-noise ratio for this SC-FSK modulation uplink is 40-dB. Thus we have a margin of 20-dB for the uplink.

Laser Safety

The worse case laser intensity at the shuttle was calculated and compared to the safe limits for our wavelength and pulse format. We are operating at 852-nm with a pulse-duration of ~ 2-ms and a repetition rate of 250-Hz. The chair of the ANSI Standard Committee on Laser Safety verified that 2-mW/cm^2 is the maximum safe exposure limit. This is to be compared to the worse case calculated intensity at the shuttle is 3-μW/cm^2, when the shuttle is at Zenith and the transmitted laser power is at a maximum. In summary, the laser intensity at the shuttle is nearly a factor of 1000 below the maximum ANSI safe exposure limit. There, we will be completely safe.

Conclusion

This simple analysis shows that a passive optical communications system that we call LOWCAL can provide a telemetering link to LEO for Zenith angles of $\pm \pi/3$. We should be able to achieve a data rate of 10-kbps over this entire range using a transmitter laser power of about 200-mW. The planned experiment will use the Advanced Pointing Telescope Facility at WSMR. Furthermore, we have presented for the first time the circular polarization keying format for free-space optical communications and the Lightwire concept that allows full-duplex communications using a single optical beam. Finally, there is absolutely no eye safety hazard for the shuttle astronauts because of the transmitter laser.

Acknowledgments

This research was supported by NASA grant NAG5-9323. The authors wish to thank Dr. Warner Miller, Dr. Steven Horan, and Dr. Robert Fugate for helpful technical discussions.

References

1. D. J. Dick and T. M. Shay, "Ultra-High Noise Rejection Optical Filter," Optics Letters, 16, p. 867, June 1991.
2. B. Yin and T. M. Shay, "Theoretical Model of Faraday Anomalous Dispersion Optical Filter," Optics Letters, 16, pp. 1617-1619, October 1991.
3. "Faraday Anomalous Dispersion Optical Filter in Potassium," with B. Yin. Optics Communications, 94, pp. 30-32, Nov. 1992.
4. "Faraday Anomalous Dispersion Optical Filter for the Cs 455 nm Transition," with B. Yin.

Photonics Technology Letters, 4, 488, May, 1992.
5. "A Sunlight Insensitive Direct Detection Optical Communications System," with L. Chen, L. S. Alvarez, Y. F. Wu, and B. Yin, Proceedings of the SPIE, 2123, pp. 448-454, 1994.
6. "Circular Polarization Keying," T. M. Shay and D. A. Hazzard, patent pending.
7. D. L. Fried, "Optical Resolution through a randomly inhomogeneous medium for very long and very short exposures," Journal of the Optical Society of America, 56, pp. 1372-1379, 1966.
8. Tracy, William, Shuttle Flight Information Officer, private communication. The typical uncertainties in the downtrack postion when the position vector is updated within 20 minutes of pass.
9. Wilson, K. E., Lesh, J. R., Araki, K., Arimoto, Y., "Overview of the Ground to Orbit Lasercom Demonstration," SPIE Proceedings, 2990, pp. 23-30, 1997, in Free-Space Laser Communications Technologies IX, G. Stephen Mercherle, Ed.
10. Wolfe, William L., Zissis, George J., Ed., The Infrared Handbook, Third edition, Pp. 3-71.
11. Vorflusev, Valery and Kumar, Satyendra, "Phase-Separated Composite Films for Liquid Crystal Displays," Science, 283, pp. 1903-1905, 19 March, 1999.
12. Swenson, Charles M., Steed, Clark A., DeLaRue, Imelda A., Fugate, Robert Q., "Low Power FLC-based Retro-modulator Communications System," SPIE Proceedings, 2990, pp. 296-310, in Free-Space Laser Communications Technologies IX, G. Stephen Mercherle, Ed.
13. Swenson, Charles M., private communication.
14. "Lightwire," T. M. Shay, J. A. Payne, and S. Horan, patent pending